2017

First-in-man evaluation of 124I-PGN650: A PET tracer for detecting phosphatidylserine as a biomarker of the solid tumor microenvironment

Richard Laforest
Washington University School of Medicine in St. Louis

Farrokh Dehdashti
Washington University School of Medicine in St. Louis

Yongjian Liu
Washington University School of Medicine in St. Louis

Jennifer Frye
Washington University School of Medicine in St. Louis

Sarah Frye
Washington University School of Medicine in St. Louis

See next page for additional authors

Molecular Imaging
Volume 16: 1-9

DOI: 10.1177/1536012117733349
journals.sagepub.com/home/mix
SAGE

First-in-Man Evaluation of ^{124}I-PGN650: A PET Tracer for Detecting Phosphatidylserine as a Biomarker of the Solid Tumor Microenvironment

Richard Laforest, PhD[1,2,3], Farrokh Dehdashti, MD[2,3], Yongjian Liu, PhD[1,2], Jennifer Frye, CMMT[3], Sarah Frye, CMMT[3], Hannah Luehmann[1], Deborah Sultan[1], Joseph S. Shan, PhD[4], Bruce D. Freimark, PhD[4], and Barry A. Siegel, MD[2,3]

Abstract

Purpose: PGN650 is a F(ab′)$_2$ antibody fragment that targets phosphatidylserine (PS), a marker normally absent that becomes exposed on tumor cells and tumor vasculature in response to oxidative stress and increases in response to therapy. PGN650 was labeled with ^{124}I to create a positron emission tomography (PET) agent as an in vivo biomarker for tumor microenvironment and response to therapy. In this phase 0 study, we evaluated the pharmacokinetics, safety, radiation dosimetry, and tumor targeting of this tracer in a cohort of patients with cancer.

Methods: Eleven patients with known solid tumors received approximately 140 MBq (3.8 mCi) ^{124}I-PGN650 intravenously and underwent positron emission tomography–computed tomography (PET/CT) approximately 1 hour, 3 hours, and either 24 hours or 48 hours later to establish tracer kinetics for the purpose of calculating radiation dosimetry (from integration of the organ time-activity curves and OLINDA/EXM using the adult male and female models).

Results: Known tumor foci demonstrated mildly increased uptake, with the highest activity at the latest imaging time. There were no unexpected adverse events. The liver was the organ receiving the highest radiation dose (0.77 mGy/MBq); the effective dose was 0.41 mSv/MBq.

Conclusion: Although ^{124}I-PGN650 is safe for human PET imaging, the tumor targeting with this agent in patients was less than previously observed in animal studies.

Keywords
PET, apoptosis, dosimetry, human imaging, cancer

Introduction

Phosphatidylserine (PS) is a cell membrane glycerophospholipid. The PS molecules normally face the cell interior but flip to the outer surface of cells during cellular stress, apoptosis, necrosis, and in response to stress conditions such as hypoxia, acidity, thrombin, inflammatory cytokines, and reactive oxygen species, which all occur in the tumor microenvironment. Thus, a PS targeting antibody could have widespread applicability as a noninvasive, in vivo imaging agent in both experimental animal models and in human diseases, including diabetes, cardiovascular disease,[1,2] and in particular cancer.[3,4] Oncology is a particularly compelling field of interest since many treatment approaches, including chemotherapy and radiotherapy, enhance PS exposure on cell membranes of

[1] Division of Radiological Sciences, Mallinckrodt Institute of Radiology, Washington University School of Medicine, St Louis, MO, USA
[2] Alvin J. Siteman Cancer Center, Washington University School of Medicine, St Louis, MO, USA
[3] Division of Nuclear Medicine, Mallinckrodt Institute of Radiology, Washington University School of Medicine, St Louis, MO, USA
[4] Peregrine Pharmaceuticals Inc, Tustin, CA, USA

Submitted: 02/05/2017. Revised: 17/08/2017. Accepted: 20/08/2017.

Corresponding Author:
Richard Laforest, Mallinckrodt Institute of Radiology, Washington University School of Medicine, St Louis, MO 63110, USA.
Email: laforestr@wustl.edu

tumor endothelium and tumor cells.[5-7] PS imaging could be employed as a general cancer imaging agent for detection, staging, and treatment monitoring,[8] including therapeutic approaches specifically designed to induce cancer cell apoptosis.[9,10] Early detection of PS exposure would provide the needed evidence to continue treatment and, conversely, the lack of an early effect could lead to a change in the treatment drug. A PS imaging agent would also be useful to assess the adequacy of dosing and to predict the likelihood of response with a PS-targeted therapy, such as the recently developed PS-targeting antibody bavituximab.[11]

PGN650 is a $F(ab')_2$ antibody fragment derived by pepsin digestion of a fully human immunoglobulin IgG1 (PGN635) that targets PS in tumors. Both PGN650 and bavituximab target exposed PS on tumors with high affinity, using a similar complexation with the circulating protein β-2 glycoprotein 1. Bavituximab has higher specificity for PS than does annexin V and higher affinity than many lower-molecular-weight molecules known to bind PS.[12] In preclinical studies, PGN650 has been used to image human tumor xenografts in mice with near-infrared (NIR) optical imaging and positron emission tomography (PET). The NIR dye-labeled PGN650 injected in mice with subcutaneous human U87 glioma tumors had a tumor to normal tissue probe ratio (TNR) of 2.5 at 24 hours postinjection.[13] Treatment of subcutaneous tumors with 12 Gy irradiation enhanced tumor uptake of NIR dye-labeled PGN650 with a TNR of 4.0 at 24 hours. Treatment of mice bearing orthotopic BT-474 human breast tumors with docetaxel enhanced NIR dye-labeled PGN650 uptake compared to untreated tumors.[4] ^{124}I-labeled PGN650 was shown to have similar binding activity in vitro compared to unlabeled PGN650 and to target human PC-3 subcutaneous and orthotopic tumors in mice as demonstrated by microPET.[14] Histological evaluation of tumor-bearing mice treated with NIR-labeled PGN650 showed that the imaging agent targeted tumor vasculature and tumor cells.[4,13] The purpose of article is to report on a first-in-man study, describing the pharmacokinetics, safety, radiation dosimetry, and tumor uptake of ^{124}I- PGN650.

Materials and Methods

^{124}I-PGN650 Production, Radiolabeling, and Quality Control

The ^{124}I (half-life = 4.18 days, 22.9% β^+ emission) was produced by 3D Imaging (Little Rock, Arkansas) via a ^{124}Te(p,n)^{124}I reaction. The percentage of iodide versus iodate was verified prior to radiolabeling via radio thin-layer chromatography. [^{124}I]NaI (10-15 mCi) buffered with 100 mM Na_2HPO_4 in 150 mM NaCl, pH 7.2 was added to 1.0 mg PGN650 buffered in 1× phosphate-buffered saline in the presence of 2 Iodogen beads (Fisher Science Education) in a borosilicate vial. The reaction was allowed to incubate at room temperature for 10 minutes followed by size-exclusion purification using a PD-10 desalting column. Fractions collected from the column with a radiochemical purity ≥95% were combined and transferred to a current Good Manufacturing Practice(cGMP) facility for sterile filtration and quality control testing. Preclinical use evaluations included radionuclidic identity, appearance and color, pH, filter membrane integrity, specific activity, radioactivity, radiochemical purity, strength, and bacterial endotoxin. Postclinical release testing included mass, chemical purity, identity, sterility, environment profile, radiochemical purity, and specific binding.

Patient Population

This study was conducted under an investigational new drug application (IND #115106, clinicaltrials.gov #NCT01632696) and approved by the institutional review board of Washington University School of Medicine. All patients provided written informed consent. Eleven patients (≥18 years) were studied. Eligible patients needed to have a biopsy-proven solid malignant tumor, an estimated life expectancy <5 years and at least 1 measurable tumor site as defined by Response Evaluation Criteria in Solid Tumors 1.1,[15] but with the specific modification for this PET protocol of a minimum tumor diameter of ≥1.5 cm. The median time lapse from the last chemotherapy to the injection of ^{124}I-PGN650 in our patient population was 26 days (range 5-526 days).

Animal Biodistribution and Dosimetry

Human radiation dosimetry estimates for ^{124}I-PGN650 were calculated from animal biodistribution data obtained by standard organ dissection method and were based on Medical Internal Radiation Dosimetry (MIRD) methodology. Normal C57BL/c male and female mice were injected with 9 μCi/100 μL of ^{131}I-PGN650 and euthanized at 1, 6, 12, 24, 48, 72, 96, and 144 hours following injection to establish the tracer biodistribution. Urinary and fecal excretion data were collected by placing the animals in metabolic cages. At these time points, normal organs were dissected, weighed, and counted for activity. Time-activity curves were created and normal organ residence times were calculated. The organ residence times were scaled to those for humans by the human to mouse relative organ weight method,[16] and the residence times were then entered into OLINDA/EXM version 1.1[17] to calculate radiation dose estimates for the human male and human female anthropomorphic models. The whole-body clearance (biological half-life) was measured by fitting a monoexponential decay function to the plot of the sum of the percentage injected dose (ID) in all organs as a function of time.

Human Imaging Studies

All PET imaging was performed with a Siemens Biograph-40 positron emission tomography/computed tomography (PET/CT) scanner (Siemens Heathineers, Knoxville, Tennessee). The planned dosage of approximately 140 MBq (3.8 mCi) of ^{124}I-PGN650 was administered over 5 minutes, after which patients were imaged at approximately 1 hour, ∼3 hours, and

at either 24 hours or 48 hours post-injection by a whole-body PET procedure from head to upper thigh. In order to limit radiation exposure to the thyroid that could result from the formation of free ^{124}I-iodide by the metabolism of ^{124}I-PGN650, patients received saturated potassium iodide solution, 2 drops orally 3 times per day, beginning 1 hour before ^{124}I-PGN650 administration, for a total of 8 days. At each imaging session, a spiral CT for attenuation correction (120 kVp, 50 mAs effective) was obtained from the top of the skull through the upper thighs, with the patient supine. Immediately after the attenuation CT scan, emission images beginning at the top of the skull and proceeding caudally through the upper thighs were obtained (1-10 minutes per bed position). Imaging was performed over 6 to 7 bed positions with a total imaging duration of no more than 1 hour. Images were reconstructed with 3D-Ordered-Subset Estimation-Maximization (OSEM) with 3 iterations, 24 subsets, and a post-reconstruction Gaussian filter of 5 mm.

Image Analysis

All images were evaluated subjectively by one observer for focal areas of abnormally increased uptake in the known sites of tumors and semiquantitatively using the maximum standardized uptake value (SUV_{max}) and tumor to blood ratio (T/B). The T/B ratio was determined by dividing the maximum counts of the tumor by the average counts of the blood pool. The overall image quality was graded as adequate to inadequate.

Human Dosimetry Calculations

Normal human dosimetry estimates were calculated from pharmacokinetic data obtained from whole-torso PET images. Regions of interests (ROIs) were drawn on the major organs as visible on the PET images, including liver, kidneys, blood pool (left ventricle), spleen, muscle, and thyroid. The total activity in the organ was calculated by scaling the measured organ activity concentrations to the standard adult organ weight. Analytical integration of monoexponential fits with the measured time-activity curves provided the organ residence times. Blood activity concentration was estimated from the left ventricular ROI. Total blood volume was estimated in accordance with Pearson et al.[18] Human dosimetry estimates were obtained from the residence times and OLINDA/EXM software (version 1.1, Vanderbuilt University) using the adult male and female models. Organ time-activity curves for every patient were collated to create average cumulative times curves from which average dosimetry estimates to normal adult human population were estimated. Bone marrow residence time was estimated from the blood residence time by the method of Wessels et al.[19] The left ventricle was assumed to contain 550 mL of blood and the lung blood volume was assumed to be 300 mL. Total activity accumulated in the urinary bladder was tallied and plotted over time. These data were then fitted by an uptake function $f(t) = A_o\,(1-\exp[-\lambda_{Bladder}\,t])$, with A_o the bladder filling fraction and $\lambda_{Bladder}$ the filling half-life. The bladder filling fraction and filling time were then used with the bladder voiding model in OLINDA/EXM, assuming a 2-hour voiding interval to estimate the residence time of urine in the bladder. A large ROI was drawn over the whole patient torso to evaluate the total activity within each patient at each imaging time points. The total torso residence time was obtained by analytical integration of a monoexponential fit on the whole-torso activity time-activity curve. The excreted activity (not observed in the urinary bladder) was obtained by subtracting this value from the maximum theoretical residence time (defined by the ^{124}I half-life/ln[2] and equal to 144.6 hours). The remainder of the body residence time was determined from the maximum theoretical residence time minus the whole torso and excreted residence times.

Safety Evaluation

All patients underwent measurement of vital signs (blood pressure, heart rate, respiratory rate, and temperature), clinical laboratory testing (standard hematologic and comprehensive metabolic panels that included hemoglobin, white blood cells, neutrophils, lymphocytes, platelets, creatinine, blood urea nitrogen, calcium, sodium, potassium, carbon dioxide, alanine transaminase, aspartate aminotransferase, alkaline phosphatase, total bilirubin, and albumin), urinalysis, and electrocardiography before ^{124}I-PGN650 administration and at the third imaging session (24 or 48 hours after injection).

Results

Tracer Production, Labeling, and Safety

Patient doses (n = 11) were successfully prepared following cGMP guidelines in a straightforward labeling synthesis with a simple purification strategy and robust quality control. Delivered activities of ^{124}I-PGN650 ranged from 137 to 263 MBq (mean 211 MBq). Radiochemical purity of the final product was 97 to 100%. The specific activity of the ^{124}I-PGN650 doses averaged 403 MBq/mg. The mass of injected tracer was 0.64 (0.13) mg (range 0.49-0.83 mg). All doses were sterile and free of bacterial endotoxins.

Animal Dosimetry

The animal dosimetry is detailed in supplemental data available online. In brief, tracer uptake was predominantly retained in the muscle, bone, and liver with a long circulation time in the blood, leading to highest radiation dose to the heart wall (mainly from activity in the blood pool), osteogenic cells, and bladder wall. A relatively high amount of tracer was observed to be excreted in the urine. Based on the animal dosimetry results, the administered activity was conservatively selected to be 140 MBq in order to result in an effective dose (ED) from the radiopharmaceutical and the CT component of the PET/CT imaging of no more than 50 mSv.

Table 1. Patient Demographic and Individual Patients PET Results.

Patient No./Age/Gender	Cancer Type/Target Lesion Location	Highest Visual Uptake	Tumor SUV_{max}			Blood SUV_{mean}		
			1 hour	3 hours	24/48 hours	1 hour	3 hours	24/48 hours
1/62/M	Esophageal cancer/mediastinal lymph node	None	0.54	0.19	0.31	16.44	10.17	7.70
2/67/F	Gastrointestinal primary/pelvic mass	Mild	4.90	7.20	9.10	10.0	8.40	6.44
3/56/M	Esophageal cancer/primary tumor	Mild	5.50	5.20	6.19	10.05	8.76	5.34
4/21/M	Ewing sarcoma/iliac mass	Minimal	2.90	4.33	5.52	5.31	6.71	3.08
5/61/M	Malignant melanoma/thigh soft tissue mass	Mild	4.70	5.13	4.03	10.60	8.19	4.06
6/65/M	Colon cancer/iliac lymph node	None	1.49	1.33	1.36[a]	6.27	7.29	2.23[a]
7/59/M	Lung cancer/primary tumor	Mild	6.10	4.49	4.45	10.71	10.86	9.55
8/54/F	Lung cancer/primary tumor	Mild	ND	2.5	2.2	ND	7.83	5.26
9/66/F	Hemangiosarcoma/llung mass	Minimal	4.30	4.22	2.90	11.90	10.60	6.55
10/68/M	Pleomorphic liposarcoma/pleural mass	Mild	5.70	3.70	6.91	10.52	8.62	6.11
11/33/M	Osteosarcoma/thigh mass	Mild	3.64	3.44	4.25	3.35	2.92	4.91

Abbreviations: F, female; M, male; ND, imaging was not done; PET, positron emission tomography; SUV_{max}, maximum standardized uptake value.
[a]Imaging performed 4 days after injection.

Patient Characteristics

Eleven patients (mean 56.7 [range 21-72] years of age; 7 men, 4 women) were enrolled in the study. The patient characteristics and PET results are summarized in Table 1.

Safety Evaluation

The mean (SD) administered activity was 135 (21) MBq (3.64 [0.56] mCi; range 88-155 MBq). There were no adverse or clinically detectable pharmacological effects in any of the 11 patients. No significant changes were observed in vital signs or inthe results of laboratory studies or electrocardiograms.

Positron Emission Tomography–Computed Tomography Biodistribution and Dosimetry

All patients except 1 underwent 3 imaging sessions; that 1 patient missed his first imaging session because of another appointment. Minimal to mildly increased ^{124}I-PGN650 tumor uptake was seen in 9 of the 11 patients. Overall, the tumor uptake was greatest at the latest imaging session (Table 1). The average tumor SUV_{max} was 4.02 (2.08) and the corresponding T/B ratio was 0.62 (0.41;Figure 1).

Activity was observed to be retained predominantly in the liver, spleen, and circulating blood. In some patients, a small amount of activity was seen to accumulate in the stomach wall. The thyroid showed only minimal uptake on the PET images. Figure 1 shows representative whole-body images at 1 hour, 3 hours, and 48 hours postinjection. Figure 2 presents the combined organ time-activity curves in the sampled organs along with the monoexponential fits. The initial retention fractions in the blood, liver, and kidneys were 60% of the ID, 12% ID, and 1.7% ID, respectively. A small spherical ROI covering the thyroid (as seen on CT) was drawn. The thyroid showed low uptake at approximately 0.08% ID. The blood showed a relatively slow clearance half-life of 46.2 hours with percentage retention of 65% (20%) at $\sim$ 45 minutes postinjection. The whole-body clearance biological half-life was 87 hours.

For most organs, a rapid distribution of the tracer to the organ is observed immediately after injection (chiefly reflecting activity in blood) followed by slow clearance. Liver clearance was observed with a time constant of 0.014/hour and blood clearance was observed with a biological half-life of 46 hours. Organ residence times are presented in Table 2 and the human radiation dose estimates are presented in Table 3. Because of its high retention, the liver is the organ receiving the greatest radiation dose (0.77 mGy/MBq; 2.59 rad/mCi). The gender-averaged ED was 0.41 mSv/MBq (1.52 rem/mCi).

Discussion

Positron emission tomography was chosen for PS imaging because of its high spatial resolution, high sensitivity, and quantitative capability. Several positron-emitting radionuclides were considered for PGN650 labeling, ranging in half-life from minutes to days. Matching of the radionuclide half-life to the pharmacokinetic profile of PGN650 was an important criterion for radionuclide selection. Feasible radiochemical labeling of PGN650 was also a key criterion. Taking these and other criteria (eg, availability, cost, and prior preclinical experience) into account, ^{124}I was chosen for PGN650 labeling, despite the fact that its physical half-life (100.22 hours) is longer than would be predicted to be necessary given a biological half-life of PGN650, based on mouse biodistribution data of approximately 15 hours. Secondly, there are several well-understood methods for labeling antibodies and other biomolecules with iodine radionuclides, including ^{124}I. Importantly, there is substantial reported experience on the use of ^{124}I for radiolabeling and molecular imaging in humans.[20-28] In addition, microPET imaging with ^{124}I-PGN650 in a rat tumor model demonstrated definite tumor uptake of this tracer at 24 and 48 hours with

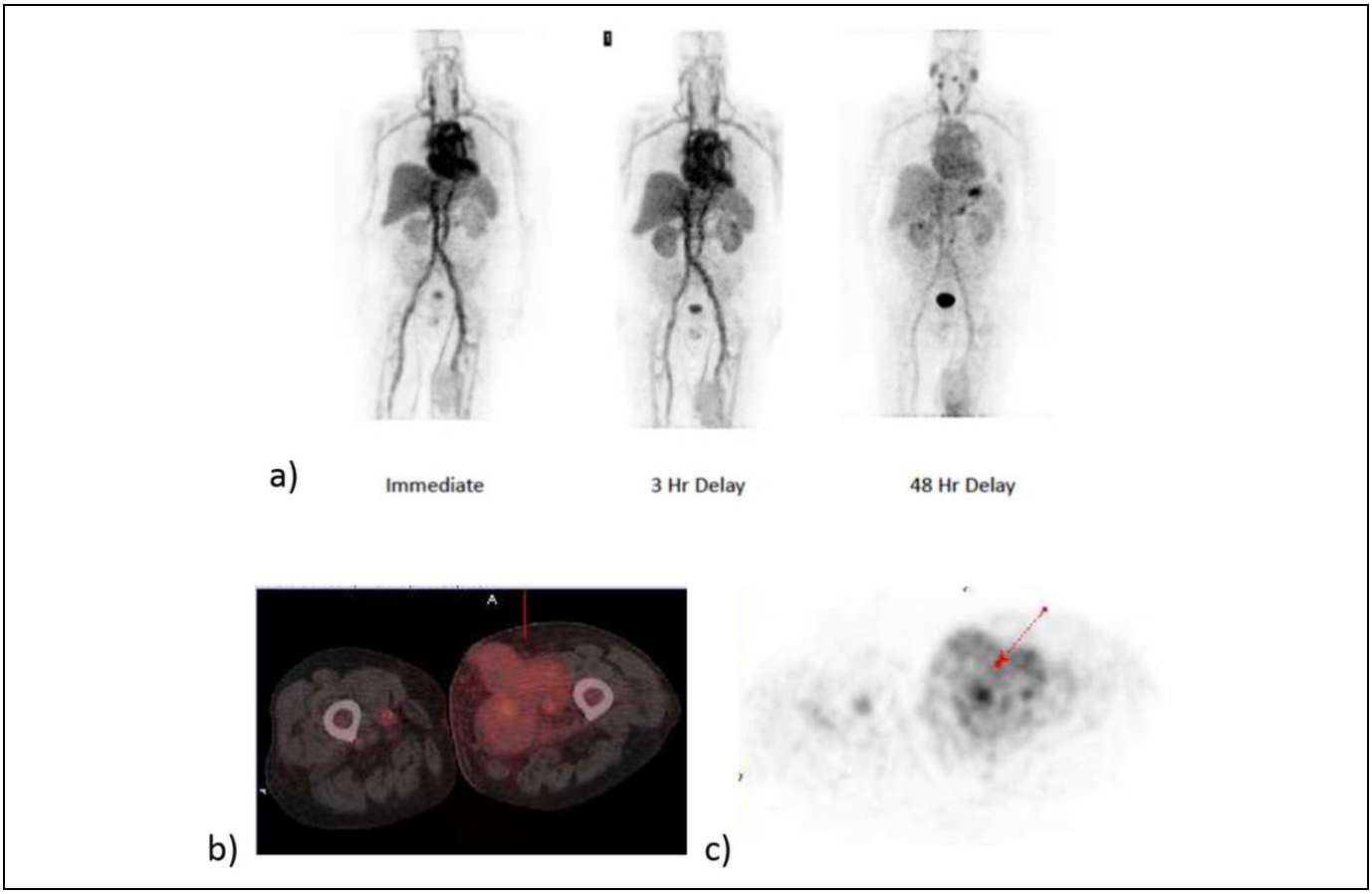

Figure 1. Representative whole-body positron emission tomography images of ^{124}I-PGN650 immediately after injection and at 3 and 48 hours' delay. Tumor uptake is observed in the left proximal thigh, see panels b and c.

acceptable nonspecific background localization, further supporting the rationale for use of ^{124}I-PGN650 imaging in humans with cancer. Although radioiodine-labeled biomolecules can suffer from in vivo deiodination, ^{124}I-PGN650 demonstrated little deiodination in the rat tumor model after potassium iodide blocking.[14] This is consistent with the lack of internalization of PS-binding antibodies in vivo and, thus, the inaccessibility to intracellular enzymes that can lead to deiodination. To our knowledge, there are no data about the pharmacokinetics of unlabeled PGN650. The mass of ^{124}I incorporated into an administered dose of PGN650 is approximately 4 ng, which is negligible compared to the mass of the PGN650 itself, and will not affect its pharmacokinetics. The results of the immunobinding assays also support the contention that there is a minimal effect of ^{124}I on the binding and biodistribution of PGN650.

The manufacturing process of ^{124}I-PGN650 was optimized to improve antigen-binding potency after it was determined that the initial manufacturing conditions (used to prepare drug product for the first 4 patients of this study) overoxidized PGN650, resulting in low immunoreactivity (antigen binding). Once these conditions were optimized, the immunoreactivity of PGN650 was found to be >85%, more comparable to that of unlabeled PGN650. However, improvement in immunoreactivity did not improve tumor uptake, likely due to the fact that tumor PS level was not increased. Increase in PS levels, which is expected to improve tumor uptake, typically occurs when therapy is combined with imaging. This was not the case in this trial.

Despite successful imaging in animal tumor models, we did not observe similar results in humans; the tumor uptake was quite low and not sufficient for clinical studies. The optimization of ^{124}I-PGN650 immunoreactivity, described above, did not have any discernible effect on tumor uptake. This low uptake, irrespective of improved immunoreactivity, is likely related, at least in part, to the fact that our patients had not had tumor-directed systemic or radiation therapy for a median of 26 days (range 5-526 days) before administration of ^{124}I-PGN650 per protocol, and thus PS exposure in the tumor did not increased above baseline. However, despite the low tracer uptake observed, the use of this approach may be relevant in future studies that include imaging before therapy, by comparison with that after therapy, where the apoptotic signal should increase if therapy is effective. A smaller antibody fragment than $F(ab')_2$, such as a minibody, might make the approach more optimal.

The tracer circulation in the blood was observed to follow a single exponential clearance function with half-life of 46.2 hours and a percentage uptake of 65% (20%) at $\sim$ 45 minutes

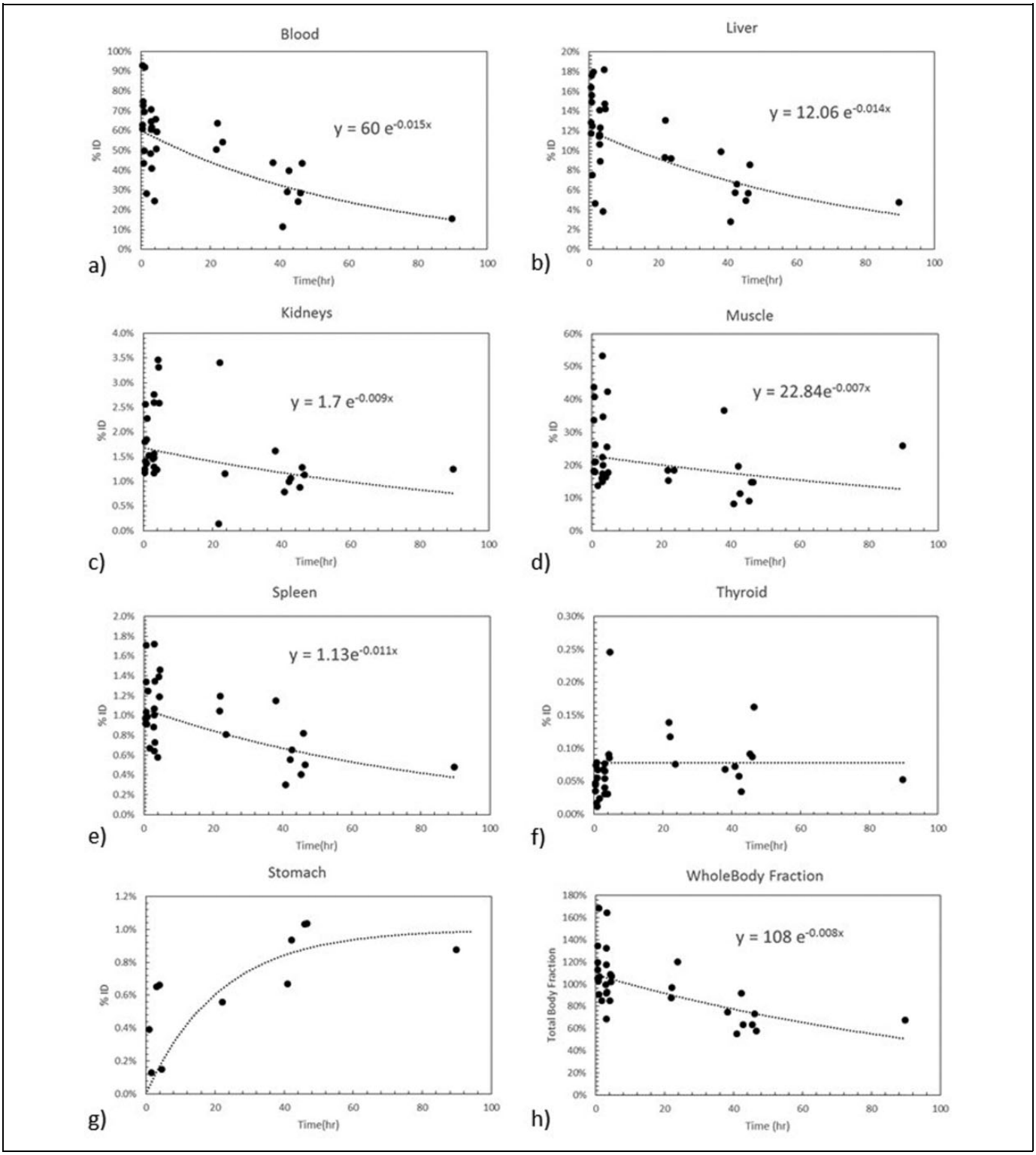

Figure 2. Cumulative organ time-activity curves obtained by collating data from all organ tracer retention from all 11 patients.

postinjection. Thus, the tracer stayed in the circulation for a sufficient time to reach and bind to the tumor. However, PS is normally expressed at low levels on tumor cells but becomes overexpressed in response to therapy that causes apoptosis. Because of the relatively long intervals between systemic or radiation therapy and imaging in our patients, the expression of PS in the tumors would be expected to be low, leading to low tumor uptake.

We evaluated the human radiation dosimetry, as well as the safety and imaging characteristics, of ^{124}I-PGN650 in an

Table 2. Organ Residence Time in Hour Derived From Whole PET/CT Image Data.

Organ	Residence Time, hours
Thyroid	0.11
Liver	5.77
Kidneys	1.06
Spleen	0.63
Blood	27.4
Muscle	16.4
Urinary bladder	0.02
Red marrow	3.80
Lungs	1.64
Heart content	2.74
Stomach	1.26
Whole body	67.0
Remainder of body	13.9

Abbreviation: PET/CT, positron emission tomography/computed tomography.

Table 3. Organ Radiation Doses for ^{124}I-PGN650 and Effective Dose From PET/CT Human Imaging.

Organ	Organ Dose Males, mGy/MBq	Organ Dose Females, mGy/MBq
Adrenals	0.28	0.36
Brain	0.10	0.19
Breasts		0.20
Gallbladder wall	0.30	0.35
Lower large intestine wall	0.17	0.27
Small intestine	0.19	0.26
Stomach wall	0.60	0.68
Upper large intestine wall	0.20	0.29
Heart wall	0.75	0.75
Kidneys	0.74	0.76
Liver	0.77	0.77
Lungs	0.40	0.44
Muscle	0.20	0.24
Ovaries		0.27
Pancreas	0.30	0.38
Red marrow	0.38	0.45
Osteogenic cells	0.32	0.50
Skin	0.11	0.16
Spleen	0.73	0.76
Testes	0.12	
Thymus	0.22	0.28
Thyroid	0.82	0.83
Urinary bladder wall	0.16	0.18
Uterus	0.18	0.26
Total body	0.21	0.28
Effective dose, mSv/MBq	0.34	0.47
Effective dose equivalent, mSv/MBq	0.41	0.40

Abbreviation: PET/CT, positron emission tomography/computed tomography.

Table 4. Comparison of Effective Dose From ^{124}I-PGN650 to Other Tracers Labeled With ^{124}I and to Other Common Nuclear Medicine Radiopharmaceuticals.

Tracer	Effective Dose, mSv/MBq
^{124}I-PGN650 (this work)	0.41
^{124}I-MIP-1095[20]	0.58
^{124}I-MIBG[22]	0.25
^{111}In-F(ab′)$_2$[29]	0.20
^{111}In-leukocytesC[30]	0.36
^{111}In-pentetreotide[29]	0.054
^{67}Ga-citrate[29]	0.10
^{64}Cu-ATSM[31]	0.036
^{89}Zr-trastuzumab[32]	0.61
^{64}Cu-DOTA-trastuzumab[33]	0.036
^{18}F-FDG[30]	0.019

Abbreviations: MIP-1095, (S)-2-(3-((S)-1-carboxy-5-(3-(4-[(124)I]iodophenyl)ureido)pentyl)ureido)pentanedioicacid, MIBG, metaiodobenzylguanidine, ASTM, diacetyl-bis(N4-methylthiosemicarbazone, DOTA, 1,4,7,10-tetraazacyclododecane-1,4,7,10-tetraacetic acid, FDG, fluorodeoxyglucose.

animal study and, subsequently, in patients. Human dosimetry estimates derived from murine biodistribution data were used to select the target ID for this human study. These data indicated a critical organ dose of 0.37 mGy/MBq (males or females) to the heart wall (reflecting the long retention time of the tracer in the blood in humans) and an average ED of 0.28 mSv/MBq (gender averaged males and females). Thus, the total ED for 3 PET/CT imaging time points for dosimetry evaluation (for 140 MBq of ^{124}I-PGN650 and 3 low-dose CT scans) was estimated to be below 50 mSv based on the preclinical dosimetry data. Since imaging is performed only up to 24 to 48 hours postinjection, ^{64}Cu might have been a better alternative to ^{124}I and would have allowed for lower radiation dose. However, for consistency with the previous preclinical studies using ^{124}I and ^{125}I, performed by the sponsor, we continued this clinical phase 0 study using the same radiolabel.

There were substantial differences between the mouse-based dosimetry extrapolated to humans and the human-based dosimetry (see Figure 3, online supplement), especially for the heart wall, kidneys, liver, and spleen. The average ED of approximately 0.28 mSv/MBq (1.04 rem/mCi) based on mouse data was lower than that based on the human data. Presumably because of the different metabolism in mice as compared to human, the tracer was observed to clear faster from the blood and was eliminated in greater proportion in urine in mice, resulting in a lower circulation time and lower liver and spleen uptake. Extrapolation of mouse dosimetry to human is not meant to provide an exact prediction of human radiation dose, but an estimate of the safe injection level for human studies.

In the human study, we observed overall longer tracer residence times in all organs. Notably the liver, kidney, and heart muscle (estimated from blood content) residence times are higher in humans, indicating slower kinetics in humans relative to rodents. Supplemental Figure S1 presents the comparative dosimetry of the animal data against the present human

dosimetry. Because of the relatively long half-life of ^{124}I and the slow clearance of the tracer in the blood, the dose to the kidneys, spleen, heart wall, and liver were determined to be approximately 0.75 mGy/MBq and the gender-averaged ED to be 0.41 mSv/MBq. An average radiation dose to the thyroid of 0.82 mGy/MBq was observed due, in part, to the thyroid blood content and also by a possible slight in vivo deiodination of the tracer in humans despite thyroid blockage with potassium iodide. It is therefore possible that deiodination is underestimated, thus explaining the high urine excretion. These radiation doses are similar to those of other cancer imaging agents labeled with ^{124}I[20] but are somewhat higher than those labeled with other radionuclides (Table 4). Patient imaging can, however, be performed safely with an injected dosage of as little as 74 MBq (2 mCi). ^{124}I-PGN650 was thus found to be safe for human imaging in this phase 0 study and no adverse effects was observed in any of our 11 patients.

Conclusion

^{124}I-PGN650 was shown to be safe for human imaging of PS, a marker of the tumor microenvironment. No adverse events were observed in the patients studied. The liver was the organ receiving the highest radiation dose at 0.77 mGy/MBq; and the gender-averaged ED was estimated at 0.41 mSv/MBq. However, tumor targeting with this agent in patients was less than previously observed in animal studies.

Acknowledgments

We want to thank Dr Steve Moerlein, PhD, PharmD, nuclear pharmacist, for prerelease quality control of the labeled product.

Declaration of Conflicting Interests

The author(s) declared the following potential conflicts of interest with respect to the research, authorship, and/or publication of this article: Joseph S. Shan and Bruce D. Freimark are employees of Peregrine Pharmaceuticals.

Funding

The author(s) disclosed receipt of the following financial support for the research, authorship, and/or publication of this article: This work was supported in part by Peregrine Pharmaceuticals Inc. (Tustin, California) and by the Alvin J. Siteman Cancer Center Imaging and Response Assessment Core.

Supplemental Material

Supplementary material for this article is available online.

References

1. Lahorte CM, Vanderheyden JL, Steinmetz N, Van de Wiele C, Dierckx RA, Slegers G. Apoptosis-detecting radioligands: current state of the art and future perspectives. *Eur J Nucl Med Mol Imaging*. 2004;31(6):887–919.
2. Belhocine TZ, Prato FS. Transbilayer phospholipids molecular imaging. *EJNMMI Res*. 2011;1(1):17.
3. Ogasawara A, Tinianow JN, Vanderbilt AN, et al. ImmunoPET imaging of phosphatidylserine in pro-apoptotic therapy treated tumor models. *Nucl Med Biol*. 2013;40(1):15–22.
4. Gong J, Archer R, Brown M, et al. Measuring response to therapy by near-infrared imaging of tumors using a phosphatidylserine-targeting antibody fragment. *Mol Imaging*. 2013;12(4):244–256.
5. Ran S, Downes A, Thorpe PE. Increased exposure of anionic phospholipids on the surface of tumor blood vessels. *Cancer Res*. 2002;62(21):6132–6140.
6. Huang X, Bennett M, Thorpe PE. A monoclonal antibody that binds anionic phospholipids on tumor blood vessels enhances the antitumor effect of docetaxel on human breast tumors in mice. *Cancer Res*. 2005;65(10):4408–4416.
7. He J, Luster TA, Thorpe PE. Radiation-enhanced vascular targeting of human lung cancers in mice with a monoclonal antibody that binds anionic phospholipids. *Clin Cancer Res*. 2007;13(17):5211–5218.
8. Belhocine T, Steinmetz N, Hustinx R, et al. Increased uptake of the apoptosis-imaging agent (99 m)Tc recombinant human Annexin V in human tumors after one course of chemotherapy as a predictor of tumor response and patient prognosis. *Clin Cancer Res*. 2002;8(9):2766–2774.
9. Blankenberg FG, Naumovski L, Tait JF, Post AM, Strauss HW. Imaging cyclophosphamide-induced intramedullary apoptosis in rats using 99mTc-radiolabeled annexin *V*. *J Nucl Med*. 2001;42(2):309–316.
10. Belhocine T, Steinmetz N, Green A, Rigo P. In vivo imaging of chemotherapy-induced apoptosis in human cancers. *Ann N Y Acad Sci*. 2003;1010:525–529.
11. Gerber DE, Stopeck AT, Wong L, et al. Phase I safety and pharmacokinetic study of bavituximab, a chimeric phosphatidylserine-targeting monoclonal antibody, in patients with advanced solid tumors. *Clin Cancer Res*. 2011;17(21):6888–6896.
12. Luster TA, He J, Huang X, et al. Plasma protein beta-2-glycoprotein 1 mediates interaction between the anti-tumor monoclonal antibody 3G4 and anionic phospholipids on endothelial cells. *J Biol Chem*. 2006;281(40):29863–29871.
13. Zhao D, Stafford JH, Zhou H, Thorpe PE. Near-infrared optical imaging of exposed phosphatidylserine in a mouse glioma model. *Transl Oncol*. 2011;4(6):355–364.
14. Stafford J H, Hao G, Best A M, Sun X, Thorpe PE. Highly specific PET imaging of prostate tumors in mice with an iodine-124-labeled antibody fragment that targets phosphatidylserine. *PLoS One*. 2013;8(12):e84864.
15. Therasse P, Arbuck SG, Eisenhauer EA, et al. New guidelines to evaluate the response to treatment in solid tumors. *J Natl Cancer Inst*. 2000;92(3):205–216.
16. Stabin MG. *Fundamentals of Nuclear Medicine Dosimetry*. New York, NY: Springer Science, Business Media; 2008.
17. Stabin MG, Sparks RB, Crowe E. OLINDA/EXM: the second-generation personal computer software for internal dose assessment in nuclear medicine. *J Nucl Med*. 2005;46(6):1023–1027.
18. Pearson TC, Guthrie DL, Simpson J, et al. Interpretation of measured red cell mass and plasma volume in adults: expert panel on

radionuclides of the international council for standardization in haematology. *Brit J Haemat*. 1995;89(4):748–756.
19. Wessels BW, Bolch WE, Bouchet LG, et al. Bone marrow dosimetry using blood-based models for radiolabeled antibody therapy: a multiinstitutional comparison. *J Nucl Med*. 2004;45(10): 1725–33.
20. Zechmann C M, Afshar-Oromieh A, Armor T, et al. Radiation dosimetry and first therapy results with a ^{124}I/^{131}I-labeled small molecule (MIP-1095) targeting PSMA for prostate cancer therapy. *Eur J Nucl Med Mol Imaging*. 2014;41(7): 1280–1292.
21. Phan HTT, Jager PL, Paans AMJ, et al. The diagnostic value of ^{124}I-PET in patients with differentiated thyroid cancer. *Eur J Nucl Med Mol Imaging*. 2008;35(5):958–965.
22. Cistaro A, Quartuccio N, Caobelli F, et al. ^{124}I-MIBG: a new promising positron-emitting radiopharmaceutical for the evaluation of neuroblastoma. *Nucl Med Rev Cent East Eur*. 2015;18(2): 102–106.
23. El-Ali HH, Eckerwall M, Skovgaard D, Larsson E, Strand SE, Kjaer A. The combination of In vivo ^{124}I-PET and CT small animal imaging for evaluation of thyroid physiology and dosimetry. *Diagnostics (Basel)*. 2012;2(2):10–22.
24. Smaldone MC, Chen DYT, Yu JQ, Plimack ER. Potential role of ^{124}I-girentuximab in the presurgical diagnosis of clear-cell renal cell cancer. *Biologics* 2012;6:395–407.
25. Khandani AH, Rathmell WK, Wallen EM, Ivanovic M. PET/CT with ^{124}I-cG250: great potential and some open questions. *AJR Am J Roentgeno*. 2014;203(2):261–262.
26. Poli GL, Bianchi C, Virotta G, et al. Radretumab radioimmunotherapy in patients with brain metastasis: a ^{124}I-L19SIP dosimetric PET study. *Cancer Immunol Res*. 2013;1(2):134–143.
27. O'Donoghue JA, Guillem JG, Schöder H, et al. Pilot study of PET imaging of ^{124}I-iodoazomycin galactopyranoside (IAZGP), a putative hypoxia imaging agent, in patients with colorectal cancer and head and neck cancer. *Eur J Nucl Med Mol Imaging Research*. 2013;3:42.
28. O'Donoghue JA, Smith-Jones PM, Humm JL, et al. ^{124}I-huA33 antibody uptake is driven by A33 antigen concentration in tissues from colorectal cancer patients imaged by immuno-PET. *J Nucl Med*. 2011;52(12):1878–1885.
29. ICRP, 2008. Radiation Dose to Patients from Radiopharmaceuticals - Addendum 3 to ICRP Publication 53. ICRP Publication 106. Ann. ICRP 38 (1-2).
30. ICRP, 1998. Radiation Dose to Patients from Radiopharmaceuticals (Addendum to ICRP Publication 53). ICRP Publication 80. Ann. ICRP 28 (3).
31. Laforest R, Dehdashti F, Lewis JS, Schwarz SW. Dosimetry of $^{60/61/62/64}$Cu-ATSM: a hypoxia imaging agent for PET. *Eur J Nucl Med Mol Imaging*. 2005;32(7):764–770.
32. Laforest R, Lapi SE, Oyama R, et al. [^{89}Zr]Trastuzumab: evaluation of radiation dosimetry, safety, and optimal imaging parameters in women with HER2-positive breast cancer, *Mol Imaging Biol*. 2016;18(6):952–959.
33. Tamura K, Kurihara H, Yonemori K, et al. ^{64}Cu-DOTA-Trastuzumab PET imaging in patients with HER2-positive breast cancer. *J Nucl Med*. 2013;54(11):1869–1875.